

Short Pulse X-Ray Laser at 32.6 nm Based on Transient Gain in Ne-like Titanium

P. V. Nickles,¹ V. N. Shlyaptsev,² M. Kalachnikov,¹ M. Schnürer,¹ I. Will,¹ and W. Sandner^{1,3}

¹Max Born Institute Berlin, Rudower Chaussee 6, 12489 Berlin, Germany

²P. N. Lebedev Physical Institute, Leninsky Prospekt 53, Moscow, Russia

³Technische Universität Berlin, Straßedes 17. Juni 135, D-10623 Berlin, Germany

(Received 11 December 1995; revised manuscript received 18 November 1996)

A novel two-step excitation scheme for an efficient table-top x-ray laser has been realized for the first time. A nanosecond pulse creates a plasma of neonlike ions of titanium, followed by a subpicosecond pulse which excites a nonstationary population inversion. With only a few joules of pump energy, a compact x-ray laser at 32.6 nm with a very high gain coefficient of $g = 19 \text{ cm}^{-1}$ and a gain-length product of $gL = 9.5$ was achieved. [S0031-9007(97)02756-7]

PACS numbers: 42.55.Vc, 52.75.Va

In recent years much effort has been directed towards the search for x-ray lasers (XRL) which are pumped by only a few joules of pulse energy from optical lasers, thus representing a so-called “table-top” system. In order to substantially reduce the pump energy requirements, various excitation schemes with one- and multiple-pulse techniques and different target geometries using laser pulses from 0.1 ns to a few ns were reported or are under development [1]. To advance into the shorter x-ray regions, the plasma has to be excited with the progressively higher flux densities; therefore, in order to keep the pump laser at a table-top size, delivering energies of $\sim 1 \text{ J}$, their pulse duration should be scaled down to the ps or fs range. Aside from excitation schemes driven by the optical field ionization in a plasma [2], the well-known recombination or collision driven XRL schemes open new possibilities for table-top XRL realizations. The main advantage of the short pulse pumping here is the creation of a transient population inversion for a collisional scheme [3], as well as the fast adiabatical cooling of the lasing medium in the case of a recombination scheme [4].

We report in this paper the first realization of a novel, effective short pulse excitation collisional scheme [3,5]. Lasing was achieved on the $3p-3s$ ($J = 0-1$) transitions of Ne-like ions at Ti XIII at a wavelength of $\lambda = 32.6 \text{ nm}$. It is characterized by a very high gain coefficient as well as a short duration and a low pumping energy. It is well known that most of the collisional x-ray lasers work in a quasisteady state (QSS) regime when the relaxation time of the excited levels is shorter than the plasma lifetime. In the limits of validity of this approximation, it is also expected to obtain beneficial properties for table-top XRL under short pulse irradiation [3,6,7]. Preliminary experiments here were already performed in [6]. The proposed approach is not based only on the pulse shortening and plasma overheating. The important difference of this concept to QSS schemes is the utilization of the advantages of short-living transient population inversion which appears due to a difference in the level excitation rates when the rise time of the excitation rates is comparable to the interatomic relaxation times [3,5]. It has been shown [3]

that, if realized, the transient scheme exhibits considerably larger gain, reaching the values of hundreds of cm^{-1} . For an x-ray laser design it is also very attractive that transient inversion can exist even in a completely optically thick plasma and does not disappear with increasing density, supposing refraction can be suppressed, thus proportionally increasing the saturation intensity and decreasing inversion lifetime. It was predicted [5] that this concept allows one, in principle, to achieve the lasing in Ne-like Ti at a pumping level of only a few joules and approach the “water window” region (2.3–4.4 nm) with Ni-like ions at 10–20 J.

Several plasma preparation methods have been proposed for utilization of transient inversion based on one- and two-step illumination of solids, foils, and low density targets (LDT) [3,5]. With LDT (foams, gaseous targets, etc.) it will be possible not only to improve heating efficiency but also to strongly reduce refraction of amplified x-rays. At the present time, one of the simplest and reliable ways is connected with the irradiation of a plane solid target. In our case, first, a relatively long 1.5 ns pulse interacts with the solid target and creates a plasma of required density, temperature, and ion composition with a substantial abundance of Ne-like Ti XIII. A second short ps laser pulse is intended to provide the temperature jump of substantial magnitude $T_e \sim \Delta E_u$ (where $\Delta E_u \sim 0.5 \text{ keV}$ is the energy of the upper laser level) for effective excitation of the Ne-like ions via electron collisions, and fast enough compared to the radiative and collisional relaxation time of the upper laser level.

Our experiments were performed at the recently upgraded CPA Nd:glass laser facility at the Max Born Institute, Berlin [8]. The large laser delivers two synchronized beams with different pulse durations. A Ti:sapphire start oscillator, followed by a stretcher and a regenerative amplifier (Spectra-Physics), is used as a 1053 nm, 1.5 ns front-end system for a linear glass amplifier chain. Before entering the power amplifier, the stretched pulse is split into two beams which are then amplified separately. One pulse is recompressed to shorter than 0.7 ps, the second one is kept at 1.5 ns duration, and the corresponding

maximum energies were 4 and 7 J, respectively. A dual cylindrical lens focusing optics enables a line focus on the target with a width of $30\ \mu\text{m}$. Typical lengths of 1–5 mm have been used in the experiments. The x-ray emission from the plasma was recorded by a transmission grating spectrograph, consisting of a toroidal mirror at grazing incidence, and a free-standing diffraction grating (2000 lines/mm). The design is similar to that reported in [9]. The nickel-covered toroidal mirror with $20 \times 81\ \text{mm}^2$ allowed one-to-one imaging of the output plane of the x-ray laser onto the recording plane. An x-ray streak camera (Kentech) with a CCS-image converter system was coupled to the spectrograph. Home designed photocathodes for the wavelength range of $\lambda > 17\ \text{nm}$ have been used in the streak camera. The streak camera was operated at a maximum temporal resolution of $\leq 10\ \text{ps}$. The spectral resolution of the whole recording system was about $0.5\ \text{nm}$.

The investigation of the amplification behavior of the Ne-like Ti scheme has shown that, with a short pulse only, no signal was observed at all. With a long prepulse at about $0.6\ \text{J}$ ($\sim 10^{11}\ \text{W}/\text{cm}^2$) in the double pulse configuration, no lasing signal was measured. Only at 4–6 J energy in the long pulse and more than 1.5 J in the 1.5 ns delayed short pulse were we able to detect a signal at 32.6 nm. It is identified as the $2p^5 3p\ ^1S_0 \rightarrow 2p^5 3s\ ^1P_1$ transition in Ne-like Ti, as observed in [10–13]. It is worth mentioning that the target geometry and the alignment of the viewing angle of the spectrograph with respect to the x-ray laser beam play an important role. By changing the angle between the target normal and the observation direction, we estimated the laser beam divergence. It was found to be within the 15 mrad acceptance angle of the spectrograph.

Figure 1 gives a streak camera record showing the temporal emission between 10–40 nm for $L = 5\ \text{mm}$ plasma

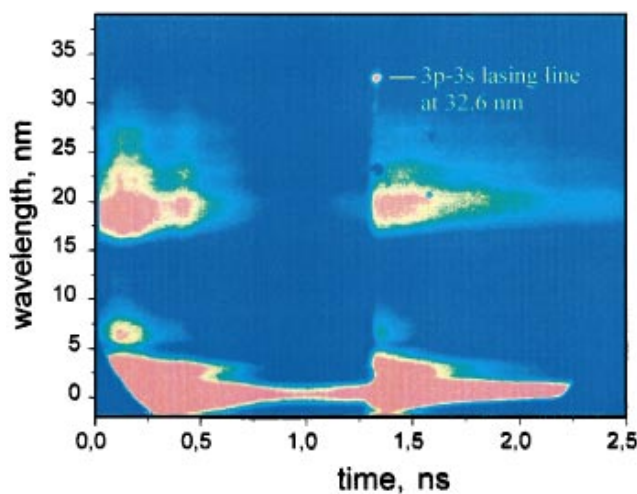


FIG. 1(color). A temporally resolved on-axis spectrum for the emission of a 5 mm Ti-plasma column produced as a result of the long (5 J) and short (2.6 J) pump irradiation, showing the bright short laser emission at 32.6 nm. The two light spots at 21 and 23 nm appear due to defects of the phosphor screen.

length at the pump intensities of $I_{p\text{-long}} = 10^{12}\ \text{W}/\text{cm}^2$ and $I_{p\text{-short}} = 10^{15}\ \text{W}/\text{cm}^2$ correspondingly. The very short and bright dot at the top which dominates the spectrum at 32.6 nm represents the $3p\text{-}3s, J = 0\text{-}1$ lasing line. In order to verify the amplification at the $3p\text{-}3s, J = 0\text{-}1$ line, we have changed the length of the plasma column (Fig. 2). The nonlinear increase of the 32.6 nm signal as a function of plasma length is clearly visible. The $3p\text{-}3s$ line intensity signals for different focal lengths of 1, 2, 3, and 5 mm at comparable pump intensities are plotted in Fig. 3. Using the Linford formula as a fit curve [14], an averaged gain for the recorded Ti-XRL pulses of $g = 19 \pm 1.4\ \text{cm}^{-1}$ was obtained. That gain is ~ 7 times more than in preceding experiments [11], utilizing a QSS regime with relatively long pulses of $\sim 0.6\ \text{ns}$ at a pump energy of 200–550 J. For the target of 5 mm in length, a gain-length product of $gL = 9.5 \pm 0.7$ was obtained. It is worth mentioning that, besides the obviously high amplification, the lasing line intensities show a substantial scatter. We find the reasons for this in our experimental conditions. The gain region has a very small lateral extension and is, additionally, characterized by a steep density gradient. Therefore the amplification is very sensitive to the plasma inhomogeneities and refraction. Investigation of the target reveals that substantial surface modifications as, e.g., groove formation following our calculations and experimental data, noticeably change the plasma hydro and refractive properties. Note, however, that at such high gain lengths the scatter in intensity by the factor of 3–20 has been characterized by many x-ray laser amplifiers [15–17].

For the approximate comparison of the efficiencies of the x-ray lasers, several relative parameters can be used [18]. Since often the size and costs of pumping facilities are restricted mainly by the energy, we adopt here from Ref. [11] the parameter gL/E_p , where E_p is the pump energy in kJ. In our case, the parameter $gL/E_p \sim 1200$, which is a factor of ~ 40 higher than in that previously reported for Ne-like Ti x-ray lasers [11].

In addition to the lasing line at 32.6 nm, we have also observed a second short living bright line at about

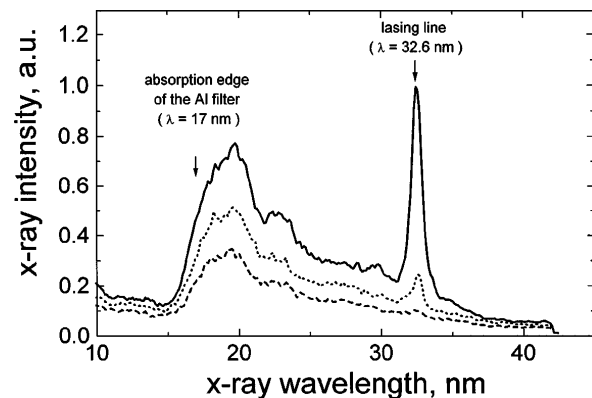


FIG. 2. Nonlinear growth of the laser signal at 32.6 nm with the plasma length of 2 mm (dotted), 3 mm (dashed), and 5 mm (solid line).

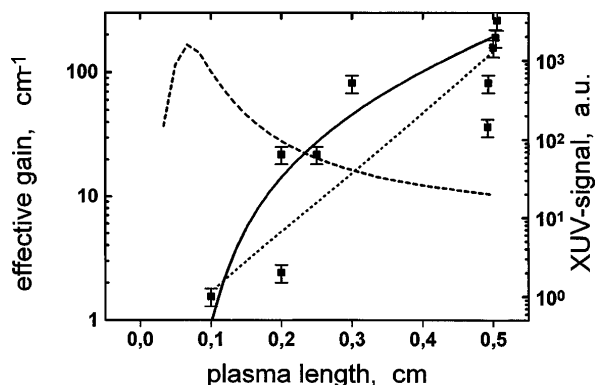


FIG. 3. XUV Intensity of the $3p-3s$, $J = 0-1$ transition in Ne-like titanium at 32.6 nm and effective gain as a function of plasma length. Solid squares: experimental values; dotted line: Linford formula fit of the experimental data with $g = 19.4 \text{ cm}^{-1}$; solid line: RADEX calculated signal intensity; dashed line: Calculated differential effective gain g_{eff} based on Linford fitting of RADEX calculated intensity. Pump laser intensity: long pulse 10^{12} W/cm^2 , short pulse 10^{15} W/cm^2 .

30 nm. It was visible only in the case of the highest pump energy and a 5 mm plasma column. Therefore we could not get data about its amplification with target length. According to the calculations, the second lasing line has been identified as a $3d-3p$, $J = 1-1$ transition of the Ne-like Ti. Its gain is predicted to reach $\sim 50\%-70\%$ of the gain of $3p-3s$, $J = 0-1$ transition. This unusual kind of inversion between $3d^1P_1$ and $3p$ levels, which appears in quasisteady state plasma with the assistance of the reabsorption of the $3d^1P_1-2p^1S_0$ transition, was already previously predicted [19,20] and experimentally observed in Ar at the long laser pulse illumination [21]. In the case of fast excitation, calculations reveal the substantial contribution of the transient inversion for the $3d-3p$ line since the large difference in excitation rates and relaxation times for $3d^1P_1$ and all $3p$ levels. An additional important property of this lasing transition is its saturation intensity which is several times larger than a $3p-3s$ transition. Our atomic data, obtained by ATOM/MZ codes [22] which were utilized for kinetics calculations [3,5,16,17,19], give a wavelength for this $3d^1P_1-3p^1P_1$ transition to 29.97 nm. Atomic data based on the HULLAC calculations [23] gives 29.61 nm, Ref. [24] predicts 29.09 nm, and the experiments [25] give 30.26 and 30.12 nm, respectively. The x-ray emission, not corrected for time resolution of the streak camera, lasts in both $3p-3s$ and $3d-3p$ lines for ~ 20 and ~ 15 ps, respectively [26]. This is the shortest pulse duration ever reported from a collisional x-ray laser. Though not measured directly, the pulse duration in the experiment described in [2] may appear in a similar range. Since the inversion exists during < 15 ps, the signal duration, corrected by inversion lifetime, should mostly correlate with the photon propagation time $L/c \sim 15$ ps (c is the speed of light) through the plasma column.

For modeling of the hydrodynamics, kinetics, and spectral properties of the transient x-ray laser, the numerical code RADEX has been used [3,5,16,17,19,27]. The model includes two-temperature 1D hydrodynamics with detailed nonlocal thermal equilibrium (LTE) atomic physics based on [22,23] and radiation transport treated self-consistently in the transient approximation. For a correct description of the amplified spontaneous emission at rapidly changing conditions, a 3D ray tracing model was developed in the time-dependent radiation transport approximation (compared to QSS in Ref. [17]) in order to take into account the effect of the finite photon transit time [28,29]. The model now allows one to calculate the whole laser-target scenario of our two pump pulse x-ray laser experiments.

The two-step irradiation scheme for the experiments with transient inversion has been proposed in [3] to reduce the plasma density in order to match the inversion relaxation time and the plasma lifetime. The plasma containing active ions should be preliminarily prepared since the inversion lifetime is usually shorter than the ionization time. Additionally, this eliminates very steep micron-scale density gradients in the case when a solid target is irradiated only by a single ps pulse.

However, as it was revealed by modeling, two main reasons play a detrimental role on the amplification in our case. First, the density gradients under sharp focusing by the ns laser pulse are very abrupt. It is also well known that, at the irradiation of solids by ns pulses, the density gradients are too strong, so in a QSS situation there was no lasing in Ti without an additional prepulse to reduce refraction and increase the amplification length [11–13]. Calculated ray trajectories of the x-ray laser beams revealed that the refraction stops amplification in the high gain area $n_e > (2-10) \times 10^{20} \text{ cm}^{-3}$ at a length of $L \sim 1-3$ mm. So despite much smaller active plasma lengths $L \sim 5$ mm than in QSS collisional schemes, the refraction here remains very important.

The second reason is a conjunctive effect of the fast transient nature of atomic kinetics of multicharged ions at the finite photon transit time during amplification $\sim L/c$. To illustrate this, the RADEX hydro code was used to calculate the process of a temperature jump formation in the plasma of the Ti target. The temperature created by ns laser prior to the short-pulse irradiation reaches values of $T_e 120-180$ eV, sufficient to ionize the plasma up to a Ne-like stage. Then the ps laser pulse heats the plasma and deposits most of the absorbed energy near the critical density $n_c = 10^{21} \text{ cm}^{-3}$, increasing locally the electron temperature to $T_e \sim 2-3$ keV. The strong saturated heat flux [27] and ionization decrease this high temperature to the $T_e \sim 0.4-0.6$ keV range during the first ~ 10 ps. After that, the cooling down to the initial temperature, due to dissipative effects, radiation, ionization, and expansion, goes slowly and takes ~ 200 ps. The transient $J = 0-1$ gain is very inhomogeneous in space and time, reaching values of $g = 50-200 \text{ cm}^{-1}$ (during 5–10 ps) in the areas

of relatively flat density profile and $\sim 500 \text{ cm}^{-1}$ (during 1–2 ps) near the critical density. Note that during the ps pulse irradiation in the thin 1–5 μm and dense ablative layer the transient gain approaches gigantic values of $\sim 10^3 \text{ cm}^{-1}$; however, for its utilization the technique of traveling wave illumination [28] and a less refracting medium are required. For comparison, a usual QSS gain is 3–10 times smaller. The short inversion lifetime in the high density area near n_c decreases the effective amplification length to $\sim 0.3\text{--}0.5 \text{ mm}$. As a result, this effect, together with refraction and collisional line broadening, substantially decreases the gain-length product and makes the peripheral regions with lower density $n_e \sim 0.7\text{--}1.5 \times 10^{20} \text{ cm}^{-3}$, smaller local gain $\sim 40\text{--}60 \text{ cm}^{-1}$, and longer inversion lifetime 10–20 ps more favorable for amplification. At the current experimental setup, without a low-energy prepulse [11–13] and traveling wave illumination, these effects restrict the effective medium to a length of $\sim 3 \text{ mm}$ (see Fig. 3).

The results of RADEX calculations of the output x-ray laser intensity, summarized in Fig. 3, very clearly reflect the present experimental situation. The effective differential gain $g_{\text{eff}} = f(L)$ has values $\sim 100 \text{ cm}^{-1}$ at the shorter lengths $L < 1 \text{ mm}$ and then decreases to $\sim 10 \text{ cm}^{-1}$ at the exit of laser amplifier $L = 5 \text{ mm}$. The processes of real intensity saturation [17] were excluded in this example to emphasize the formation of the saturationlike intensity behavior due to refraction and time-dependent effects. Integration of the calculated g_{eff} over the length gives $g_{\text{eff}}L \sim 15.5$ which is just 1.5–3 units less than the saturation limit. The experimental gL reported here is smaller than this value since, for the reliable resolution of such intensity behavior, much more measurements are required, particularly at the shorter lengths. Nevertheless, the indications that the actual gL in our experiment might be larger clearly exist (Fig. 3). At the saturation, it is expected to extract the energy on the level of units of μJ . With its existing potential in further reduction of the pumping energy to sub-J range [3,5], this scheme will deliver ultimate efficiency in this spectral range. Detailed investigation of the questions of achievement of the saturation limit, based on this and very recent experimental material and the present numerical model, we will address in a future publication.

In summary, we have experimentally verified the previously predicted transient inversion collisional x-ray laser concept [3,5]. The key element of this concept, the utilization of short-living enhanced population inversion, appears ideally suited for modern short-pulse CPA pump lasers. A gain of 19 cm^{-1} and a gain-length product of 9.5 were obtained. This highly efficient, small sized x-ray laser, based on Ne-like titanium, exhibited a wavelength of 32.6 nm, a pulse duration of less than $\sim 20 \text{ ps}$, and is characterized by a drastic reduction of pump energy (only a few joules) compared to the classical collisional XRL. It is anticipated that, after this proof of principle experiment, this concept will lead towards saturated compact

collisional x-ray lasers delivering substantial energy and working at a much shorter wavelength and pulse duration.

We gratefully acknowledge the help of A. L. Osterheld for discussions and providing the atomic data for Ne-like Ti, and J. Nilsen for useful references. This work was partially supported by the European x-ray laser TMR network.

-
- [1] P. Hagelstein *et al.*, SPIE **2012**, 88 (1993); T. Hara *et al.*, *ibid.*, 217 (1993); A. Morozov *et al.*, *ibid.*, 180 (1993).
 - [2] N.H. Burnett and P.B. Corkum, J. Opt. Soc. Am. B **6**, 1195 (1989); P. Amendt *et al.*, Rev. A **45**, 6761 (1993); B.E. Lemoff *et al.*, Opt. Lett. **19**, 569 (1994); Y. Nagata *et al.*, Phys. Rev. Lett. **71**, 3774 (1993); B.E. Lemoff *et al.*, Phys. Rev. Lett. **74**, 1574 (1995); B.N. Chichkov *et al.*, Phys. Rev. A **52**, 1629 (1995).
 - [3] Yu.A. Afanasiev and V.N. Shlyaptsev, Sov. J. Quantum Electron. **19**, 1606 (1989); *Proceedings of the International Symposium on Short-Wave Lasers, Samarkand, 1990* (Nova Science, New York, 1992), p. 197; P.N. Levedev Phys. Institute, Moscow Report No. 40, 1985; V.N. Shlyaptsev, Ph.D. thesis, P.N. Levedev Phys. Institute, Moscow 1987 (in Russian) (unpublished); V.N. Shlyaptsev and A.V. Gerusov, in *Proceedings of the 3rd International Coll. on X-Ray Laser, Schliersee, Germany, 1992* (IOP, Bristol, 1992), p. 195.
 - [4] J. Zhang *et al.*, Phys. Rev. Lett. **74**, 1335 (1995).
 - [5] V.N. Shlyaptsev, P.V. Nickles, T. Schlegel, M.P. Kalashnikov, and A.L. Osterheld, SPIE **2012**, 111 (1993).
 - [6] L.B. Da Silva *et al.*, SPIE **1229**, 128 (1990).
 - [7] S. Maxon *et al.*, Phys. Rev. Lett. **70**, 2285 (1993).
 - [8] M.P. Kalashnikov *et al.*, Laser Part. Beams **12**, 463 (1994).
 - [9] J. Jasny *et al.*, Rev. Sci. Instrum. **65**, 1631 (1994).
 - [10] E. Träbert, Z. Phys. D **1**, 283 (1986).
 - [11] T. Boehly *et al.*, Phys. Rev. A **42**, 6962 (1990).
 - [12] J. Nilsen *et al.*, Phys. Rev. A **48**, 4682 (1993).
 - [13] E.E. Fill *et al.*, SPIE **2520**, 134 (1995).
 - [14] G.J. Linford *et al.*, Appl. Opt. **13**, 397 (1974).
 - [15] B.J. MacGowan *et al.*, Phys. Fluids B **4**, 2326 (1992).
 - [16] J.J. Rocca *et al.*, Phys. Rev. Lett. **73**, 2192 (1994).
 - [17] J.J. Rocca *et al.*, Phys. Rev. Lett. **77**, 1476 (1996); F.G. Tomasel *et al.*, Phys. Rev. A **54**, 2474 (1996).
 - [18] R.C. Elton, *X-Ray Laser* (Academic Press, New York, 1990).
 - [19] A.V. Vinogradov and V.N. Shlyaptsev, Sov. J. Quantum Electron. **14**, 303 (1983).
 - [20] J. Nilsen, Phys. Rev. A **53**, 4539 (1996).
 - [21] H. Fiedorowicz *et al.*, Phys. Rev. Lett. **76**, 415 (1996).
 - [22] L.A. Vainshtein and V.P. Shevelko, *Atomic Physics for Hot Plasmas* (Inst. of Phys. Pub., Bristol, 1993).
 - [23] A.L. Osterheld (private communications).
 - [24] A.K. Bhatia *et al.*, At. Data Nucl. Data Tables **32**, 435 (1985).
 - [25] J.-P. Buchet *et al.*, J. Phys. B **20**, 1709 (1986); C. Jupen, Phys. Scr. **53**, 139 (1996).
 - [26] P.V. Nickles *et al.*, SPIE **2520**, 373 (1995).
 - [27] Yu. V. Afanasiev *et al.*, J. Sov. Laser Res. **10**, 1 (1989).
 - [28] J.C. Moreno *et al.*, Opt. Commun. **110**, 585 (1994).
 - [29] J.A. Koch *et al.*, Phys. Rev. A **50**, 1877 (1994).